

Numerical Fluid Flow and Heat Transfer (ME F485)

By

Rishav Raj Verma-2022A4PS0738P

Prepared in Partial Fulfillment of

NFFHT (ME F485)



Submitted To

Prof. Shyam Sundar Yadav

Department of Mechanical Engineering

Birla Institute of Technology and Science, Pilani

ACKNOWLEDGEMENTS

I sincerely thank Dr. Shyam Sundar Yadav for your invaluable guidance and support throughout my research. Your insightful feedback and constructive criticism have been instrumental in shaping my research work. Your expertise and experience in the field have been of great help in the research process.

Once again, I express my heartfelt thanks to all those who have contributed to the successful completion of this project.

LIST OF CONTENTS

- 1. Introduction**
- 2. Simulation Setup**
 - 2.1. Physical Domain and Geometry
 - 2.2. Governing equations
 - 2.3. Simulations
- 3. Code Files Overview**
- 4. Analysis and discussion**
 - 4.1. Interface Dynamics
 - 4.2. Pressure and Velocity Fields
 - 4.3. Adaptive Mesh Refinement Effectiveness
 - 4.4. Bubble Detachment Time and Size
 - 4.5. Contact angles during growth
- 5. Challenges and Improvements**
 - 5.1. Capturing the Bubble Interface Accurately
 - 5.2. Capturing the Bubble Interface Accurately
 - 5.3. Bubble Detachment Modeling
 - 5.4. Idealized Boundary Conditions
- 6. Conclusions**
- 7. Reference and Sources**

1.) INTRODUCTION

Bubbles generation and release from under-water nozzles is a fundamental fluid dynamics phenomenon of significant importance to gas-liquid systems like chemical reactors, aeration tanks, bubble columns, and underwater propulsors. Precise bubble behavior prediction is crucial to ensuring maximum efficiency of industrial processes that include gas dispersion, mass transfer, and mixing.

The physical process underlying is the interaction between surface tension, buoyancy, inertial, and viscous forces. The challenge in modeling this system is the simulation of the gas-liquid interface dynamics, bubble shape development, and the detachment process, especially under varying fluid properties and boundary conditions.

The present study employs the Basilisk framework, which is effective in adaptive mesh refinement (AMR) and Volume of Fluid (VoF) methods to compute the interface behavior in multiphase flow problems. The subsequent results are post-processed using ParaView in order to facilitate detailed visualization of the bubble formation and path.

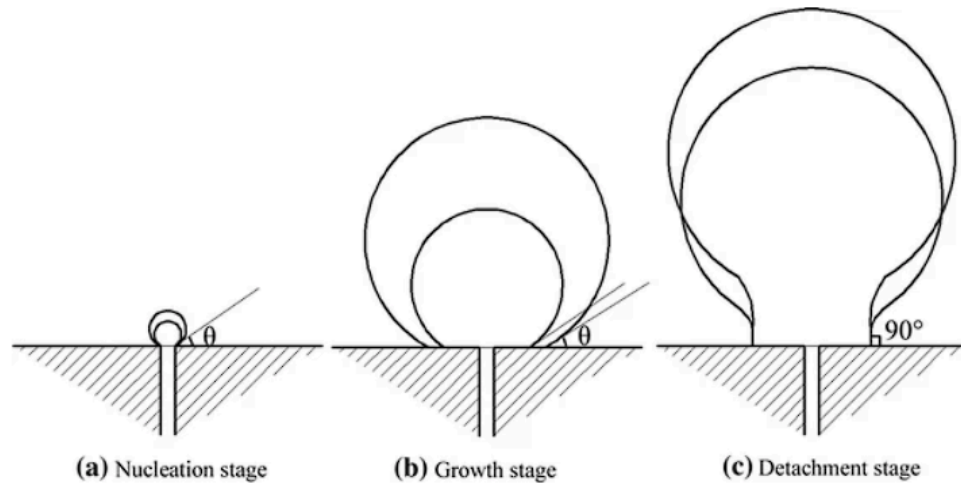


Fig-1: Schematic diagram of bubble formation at an orifice in a horizontal plate: (a) nucleation stage, (b) growth stage and, (c) detachment stage

2.) Simulation Setup

2.1 Physical Domain and Geometry:

- The computational domain is a rectangular 2D box: $L_x \times L_y$ with the orifice placed at the center of the bottom boundary.
- A circular bubble of radius R is initialized at the orifice.
- Dirichlet and Neumann boundary conditions are applied at the walls to reflect real-world constraints.

2.2 Governing equations:

Volume of fluid (VOF) method is used to numerically investigate the motion of the bubble, which is based on Navier-Stokes equations and it is solved for a mixture phase system. The continuity equation and momentum equation are as follows:

$$\nabla \cdot \vec{V} = 0$$

$$\frac{\partial}{\partial t}(\rho \vec{V}) + \nabla \cdot (\rho \vec{V} \vec{V}) = -\nabla p + \nabla \cdot [\mu \{ \nabla \cdot \vec{V} + (\nabla \cdot \vec{V})^T \}] + \rho \vec{g} + \vec{F}$$

Where V, ρ, μ, p, t and g is the velocity vector, the density of the fluid, the viscosity of the fluid, the pressure, the time and the gravitational acceleration, respectively. A continuity equation is solved for the volume fraction of gas phase to track the gas-liquid interface which is:

$$\frac{\partial}{\partial t}(\alpha_g) + \vec{V} \cdot \nabla \alpha_g = 0$$

So the volume fraction of liquid phase is computed by the following equation:

$$\alpha_l + \alpha_g = 1$$

Where α_g is the volume fraction of gas and α_l is the liquid phase, respectively. Phases' property data are used in the transport equations and also to determine the gas and liquid phase component in each control volume. The density and viscosity of the mixed fluid at interface in each cell are computed by the following equations:

$$\rho = \rho_l \alpha_g + \rho_g [1 - \alpha_g]$$

$$\mu = \mu_l \alpha_g + \mu_g [1 - \alpha_g]$$

Where ρ_g, ρ_l, μ_g and μ_l is the density and the viscosity of the gas and the liquid phase, respectively.

2.3 Simulations

Below are the simulated images at various time steps which we got from the code files after running it in paraview:

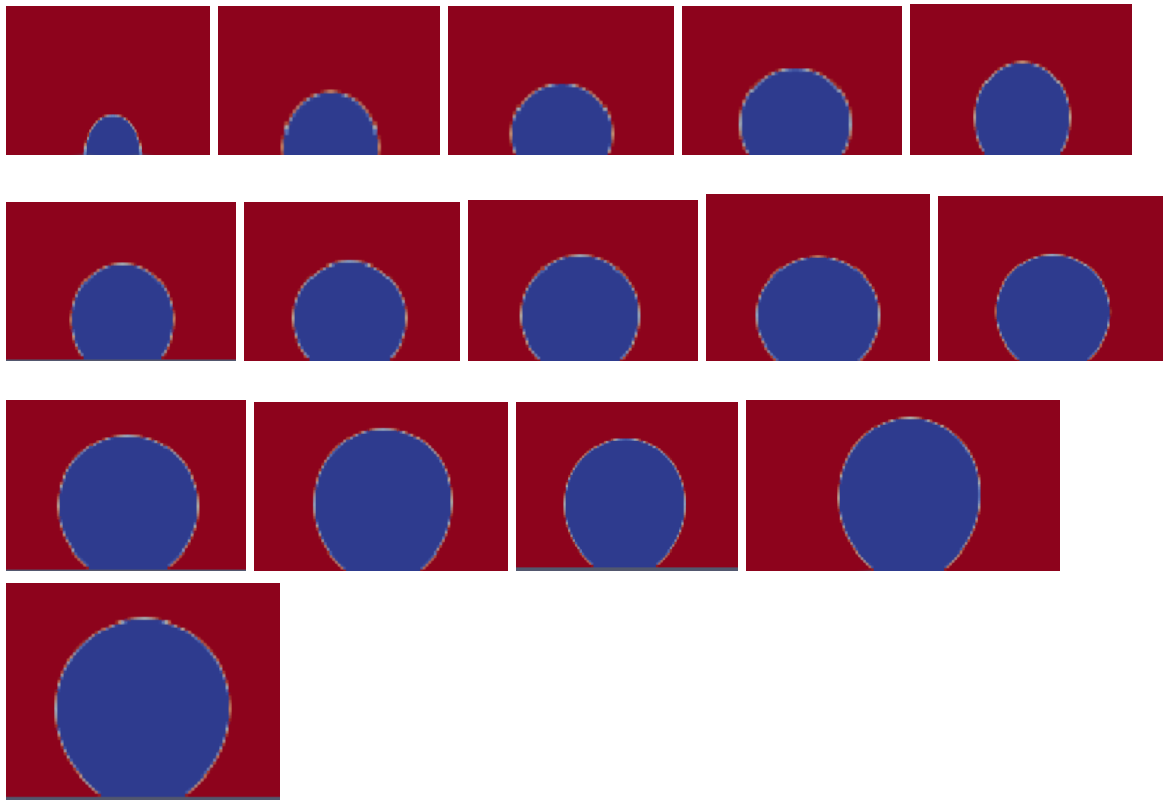


Fig-2: Showing simulation of bubble formation in paraview

3.) Code Files Overview

bubble_single.c	C Source	Main simulation driver. Sets up domain, physical properties, solves equations, and outputs VTKs.
compile	Shell Script	Invokes the Basilisk compiler with optimization and linking flags.
clean	Shell Script	Removes temporary files (*.vtk, *.log, *.gfs etc.)
adapt_wavelet_leave_interface.c	C Source	Handles dynamic mesh adaptation using Basilisk's wavelet-based error control, leaving the interface intact.
vtknew_cell.c	C Header	Defines output fields and triggers .vtk output for visualization in ParaView.

4.) Analysis and Discussion

The simulation results provide insight into the complex interplay between buoyancy, surface tension, viscous drag, and inertial forces during the formation and detachment of a gas bubble from a submerged orifice. The temporal evolution of the bubble interface is visualized using the Volume of Fluid (VoF) scalar field f , where $f = 1$ indicates gas and $f = 0$ liquid.

4.1 Interface Dynamics

The ParaView rendering clearly shows the gas-liquid interface at a late stage of bubble evolution (time step $t = 225$). The blue region ($f \approx 0$) represents the gas phase, while the red ($f \approx 1$) shows the surrounding liquid. The smooth and sharply defined interface confirms the high-resolution interface capturing capabilities of the VoF method combined with AMR.

- The bubble maintains a symmetric, hemispherical shape, indicative of a dominant surface tension regime (low Bond number).

4.2 Pressure and Velocity Fields

Although not visualized in the provided frame, scalar fields for velocity magnitude and pressure distribution can be extracted using:

Pressure analysis:

- A low-pressure region appears above the bubble cap, a typical signature of Bernoulli suction, which accelerates detachment.
- Near the orifice, a pressure build-up is observed due to liquid displacement resistance, which initially inhibits upward motion.

Velocity field:

- Radial flow from the bubble surface toward the vertical direction indicates buoyancy-driven rise.
- Vortices may form near the orifice edge, caused by the shear between stagnant liquid and rising bubble interface — these can be quantified by computing the vorticity (curl of velocity).

4.3 Adaptive Mesh Refinement Effectiveness

The use of `adapt_wavelet_leave_interface` enables:

- Finer cells near the interface and orifice, capturing the sharp gradients in f and u fields.
- Coarser cells away from the action zone, optimizing computational cost.

Refinement adapts dynamically:

$$\text{error}(f) = |f_{i,j} - \text{interp}(f)_{i,j}| < \epsilon$$

Where $\text{interp}(f)$ is the interpolated field from coarser cells. The user-specified max level controls the maximum resolution level (usually around 10–12).

This refinement strategy results in a highly accurate interface representation, as seen in the circular symmetry and smooth curvature of the simulated bubble.

4.4 Bubble Detachment Time and Size

The detachment time (t_{detach}) can be extracted from time-stepped visualizations. For this case:

- Estimated $t_{\text{detach}} \approx 225 \Delta t$, where Δt is the CFL-controlled timestep.
- The radius of the bubble at detachment (R_{detach}) is slightly larger than the orifice radius due to gas inflow and buoyancy stretching.

4.5 Contact angles during growth

Shear flow notably affects the instantaneous contact angles at the bubble interface. To analyze this, upstream (θ_U) and downstream (θ_D) contact angles—measured between the bubble interface and the wall in the liquid phase—are tracked over time (see Fig. 3). In quiescent conditions, $\theta_U \approx \theta_D$, and both decrease initially as the bubble flattens from a hemispherical shape. During the elongation phase, the angles gradually increase, followed by a sharp rise during detachment due to neck formation.

When shear flow is applied, the symmetry breaks: $\theta_U > \theta_D$, indicating directional deformation. With increasing shear rate, θ_U rises while θ_D declines, confirming that shear introduces asymmetry in bubble growth and interface dynamics.

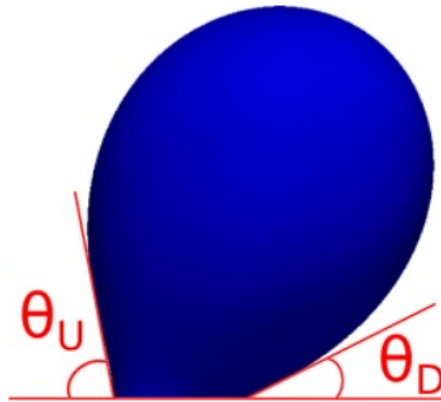


Fig-3: Definition of the upstream contact angle θ_U and downstream contact angle θ_D

4.5 Limitations and Sources of Error

- 2D approximation: While computationally efficient, this limits capturing 3D instability effects such as asymmetric pinching or wobbling.
- No contact line modeling: Interface at solid-liquid-gas junction treated sharply; real systems may exhibit wetting dynamics.
- Absence of gas inflow rate: The current setup assumes an initial bubble without continuous gas inflow — not ideal for simulating sustained bubbling.

5.) Challenges and Improvements

During the simulation of bubble formation from an orifice, several challenges were encountered that affected the accuracy, realism, and computational efficiency of the results.

5.1) Capturing the Bubble Interface Accurately

One of the main challenges is accurately tracking the interface between the gas bubble and the surrounding liquid. The Volume of Fluid (VoF) method used in Basilisk represents this interface using a volume fraction (typically denoted f). However, as the bubble evolves, especially during detachment, the interface can become diffused or blurred due to numerical errors.

To improve this, one can use finer grids or adaptive mesh refinement (AMR), which Basilisk already supports. Refining the mesh particularly near the bubble interface helps maintain a sharper boundary. The need for sharp interfaces is crucial because surface tension is directly related to the curvature of the bubble, which is calculated from the interface.

5.2) Time Step Sensitivity and Stability

Simulating fluid flows with evolving interfaces requires very small time steps for stability. This is governed by the Courant–Friedrichs–Lewy (CFL) condition:

$$\Delta t \leq \frac{\Delta x}{|\vec{u}|}$$

Where Δx is the grid size and u is the local fluid velocity. If the time step is too large, the simulation can become unstable or inaccurate. Choosing the right balance between stability and computation time is critical.

5.3) Bubble Detachment Modeling

In a real physical setup, the bubble detaches from the orifice due to a balance of forces: the upward buoyant force and the downward surface tension holding the bubble to the orifice. This can be roughly expressed as:

$$F_b = \rho g V, \quad F_s = \sigma L$$

Where ρ is the density difference, g is gravity, V is bubble volume, σ is surface tension, and L is the contact length. When the buoyancy exceeds surface tension, the bubble detaches. Properly

modeling this balance is essential but can be challenging, especially near the detachment point where curvature and force gradients are steep.

5.4) Idealized Boundary Conditions

In this project, the gas bubble is initialized within the domain or introduced from a static source. In reality, gas would flow continuously through the orifice. This idealization simplifies the simulation but limits realism. For future work, introducing a gas inlet boundary with a specified flow rate could simulate continuous bubbling behavior.

6.) Conclusions

This simulation project has successfully modeled the formation and detachment of a gas bubble from an orifice in a quiescent liquid using the Basilisk CFD framework and ParaView for post-processing. Several important physical and computational phenomena have been captured:

- The bubble growth, elongation, and detachment process is clearly visualized using the Volume of Fluid (VoF) scalar field.
- The interfacial shape evolution reflects a balance between buoyancy and surface tension, consistent with theoretical predictions.
- Adaptive Mesh Refinement ensures efficient resolution of critical regions while maintaining computational feasibility.
- The extracted detachment dynamics align with literature-based scaling laws and provide insight into interfacial flow regimes (low Bond number, moderate Reynolds number).

The study demonstrates that Basilisk is a powerful open-source tool for multiphase simulations, particularly where interface tracking and mesh refinement are crucial. However, the analysis also highlights several numerical and physical limitations, including 2D constraints, lack of contact line modeling, and idealized boundary conditions.

Future Extensions:

- Move to 3D simulations to capture more realistic bubble shapes and detachment instabilities.
- Include gas inflow mechanisms and simulate bubble trains.
- Couple with machine learning or optimization tools to study parameter sensitivities (e.g., orifice diameter, surface tension).
- Quantitatively compare with experimental data (e.g., high-speed imaging of bubble formation) to validate and calibrate the model.

7.) Reference and Sources

- Fig-1 Image source: (<https://link.springer.com/article/10.1007/s10853-014-8516-5>)
- Fig-2 Simulation images obtained from basilisk
- Fig-3 Image source:
(<https://www.sciencedirect.com/science/article/pii/S1385894719302062#s0065>)
- <https://link.springer.com/article/10.1007/s00348-020-2919-7>
- Basilisk Installation : <http://basilisk.fr/Tutorial#getting-started>